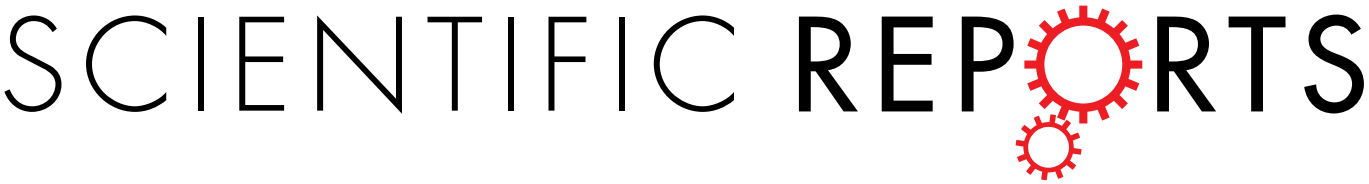

OPEN

Structural disorder in metallic glass-forming liquids

Shao-Peng Pan[1,2], Shi-Dong Feng[3], Li-Min Wang[3], Jun-Wei Qiao[1,2], Xiao-Feng Niu[1,2], Bang-Shao Dong[4], Wei-Min Wang[5] & Jing-Yu Qin[5]

Received: 29 February 2016
Accepted: 24 May 2016
Published: 09 June 2016

We investigated structural disorder by a new structural parameter, quasi-nearest atom (QNA), in atomistic configurations of eight metallic glass-forming systems generated through molecular dynamics simulations at various temperatures. Structural analysis reveals that the scaled distribution of the number of QNA appears to be an universal property of metallic liquids and the spatial distribution of the number of QNA displays to be clearly heterogeneous. Furthermore, the new parameter can be directly correlated with potential energy and structural relaxation at the atomic level. Some straightforward relationships between QNA and other properties (per-atom potential energy and α-relaxation time) are introduced to reflect structure-property relationship in metallic liquids. We believe that the new structural parameter can well reflect structure disorder in metallic liquids and play an important role in understanding various properties in metallic liquids.

Full understanding the atomic structure of metallic melts is helpful on the production of metallic materials[1–3]. However, the identification and successive analysis of atomic structure in metallic liquids is a formidable scientific challenge which is attracting constant interest[4–6]. Compared with the metallic crystals, the atomic structure of metallic melts is more disordered, which are closely correlated with various properties in metallic melts[7]. Due to a lack of the long-range order in metallic melts, it is difficult to reflect all the aspect of the atomic structure in metallic melts by several structural parameters. How to better describe the atomic structure, especially to better reflect the structure-property relationship in metallic liquids and glasses becomes the research hotspot of many physical scientists.

Previous studies have studied the structure-property relationship in metallic liquids and glasses. Icosahedral clusters have been proved to play an important role in structure-property relationship in metallic liquids and glasses[8], however, in some systems icosahedral clusters are absent[9]. The Debye-Waller factor has been quite successful for predicting the relative long-time dynamical heterogeneity[10]. The localized soft mode was used to search origin of dynamic heterogeneity in liquids[11] and deformation in metallic glasses[12]. However, both of the two characterizations cannot provide a clear picture of local atomic structure. Many works reveals that there exists some regions, where the atomic packing is rather loose or dense, in metallic glasses and these regions are closely correlated with the properties in metallic glasses[7]. However, the present structure parameters cannot effectively identify the degree of atomic packing. The free volume concept[13–15] might be one choice to describe the degree of atomic packing. However, it is impossible to measure the free volume rigorously because an atom does not have an indefinite volume[16]. Besides that, the value of free volume cannot provide any direct structure information. Therefore, although there has been some significant progress to characterize local structure, an effective parameter to directly describe and quantify the local packing in metallic liquids is still needed.

In previous work, we propose a new structural parameter, quasi-nearest atom (QNA), and found that QNA shows close correlation with dynamic heterogeneity in a metallic liquid[17]. We think that QNA can be used to describe local packing in metallic liquids. In this work, we will investigate structural disorder by QNA and its role in structure-property relationship in metallic liquids.

[1]College of Materials Science and Engineering, Taiyuan University of Technology, Taiyuan, 030024, China. [2]Shanxi key laboratory of advanced magnesium-based materials, Taiyuan University of Technology, Taiyuan, 030024, China. [3]State Key Laboratory of Metastable Materials Science and Technology, Yanshan University, Qinhuangdao, 066004, China. [4]Advanced Technology & Materials Co., Ltd., China Iron & Steel Research Institute Group, Beijing, 100081, China. [5]Key Laboratory for Liquid-Solid Structural Evolution and Processing of Materials (Ministry of Education), Shandong University, Jinan 250061, China. Correspondence and requests for materials should be addressed to S.-P.P. (email: shaopengpan@gmail.com)

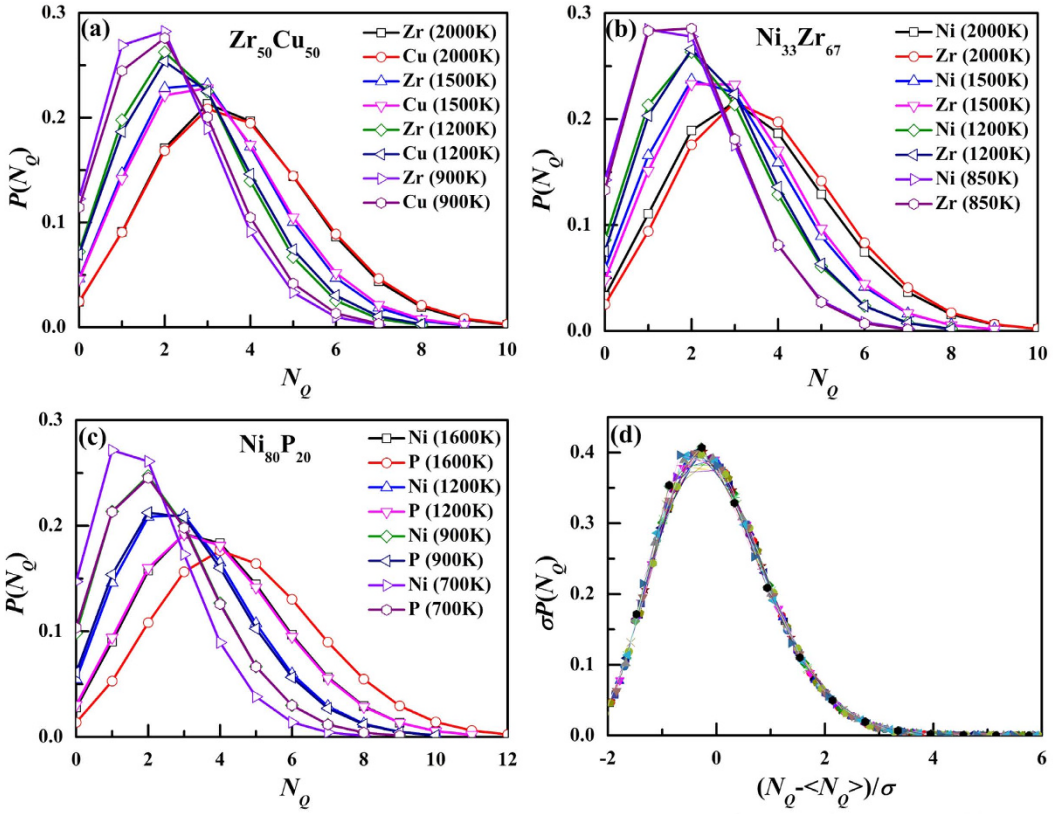

Figure 1. The temperature dependence of the distributions of N_Q in (**a**) $Zr_{50}Cu_{50}$, (**b**)$Ni_{33}Zr_{67}$ and (**c**) $Ni_{80}P_{20}$, (**d**) the distributions of N_Q, shifted by the average value $<N_Q>$ and scaled by the standard deviation σ for those in (**a–c**).

Results and Discussion

The temperature dependence of QNA. Figure 1 shows the distribution of the number of QNAs (N_Q) in three model systems. Figure 1(a) displays the distributions in $Zr_{50}Cu_{50}$, a well-known metallic system with icosahedral short range order (ISRO)[18]. At the temperature of 2000 K, 1500 K, 1200 K and 900 K, the distributions of N_Q around Zr and Cu are almost the same, indicating the similar denseness of atomic packing around Zr and Cu atoms. At 2000 K, the distributions have a peak at N_Q~3. As temperature decreases, the positions of the peaks move to smaller N_Q, suggesting that the atomic packing of the system becomes denser as temperature decreases. Figure 1(b) shows the distribution in $Ni_{33}Zr_{67}$, a metallic system with few ISRO[9]. Similar to $Zr_{50}Cu_{50}$, the distribution of N_Q around the two components are almost the same and the positions of the peaks move to smaller N_Q as temperature decreases. As shown in Fig. 1(c), the distributions of N_Q in $Ni_{80}P_{20}$, a metal-metalloid system[19], are a little different from those in $Zr_{50}Cu_{50}$ and $Ni_{33}Zr_{67}$. At each temperature, the distributions for Ni and P are quite different. The positions of peaks for P are located at larger N_Q. This fact indicates that the atomic packing around P atoms is much looser than that around Ni atoms, which is reasonable for metalloid element. Although the distributions of N_Q change as systems and temperatures, their shapes are similar. Figure 1(d) displays the distributions shifted by the average value $<N_Q>$ and scaled by the standard deviation σ for those in (a–c). This leads to the striking result that the scaled distribution of N_Q appears to be universal, which is similar to the Voronoi cell volume and asphericity[14]. The scaling of $P(N_Q)$ suggests that there might exist a single underlying geometrical structure of the system for metallic liquids with embedded atom method (EAM) potentials, and that system specifics, such as temperature and density, are absorbed into the average and variance of the distribution. The universal distribution of N_Q might be the basic property in metallic liquids. Further work should be done in more systems with other potentials for confirmation.

Figure 2 shows the temperature dependence of the average N_Q, $<N_Q>$, for eight systems. As temperature decreases, $<N_Q>$ decreases, suggesting that the atomic packing of the system becomes denser and denser. At high temperatures, $<N_Q>$ displays a linear temperature dependence. As temperature decreases, the linear correlation is deviated. Here, we proposed a power law of $<N_Q> \sim (T - T^*)^b$ to fit $<N_Q>$ as a function of temperature shown in Fig. 2(a):

$$<N_Q> = a^*(T - T^*)^b \quad (1)$$

The simulated data are fitted very well by the power-law function and the statistical correlation parameter R^2 is better than 0.99. At T^*, $<N_Q>$ should be zero, which means the system has no structural "defect" and should be

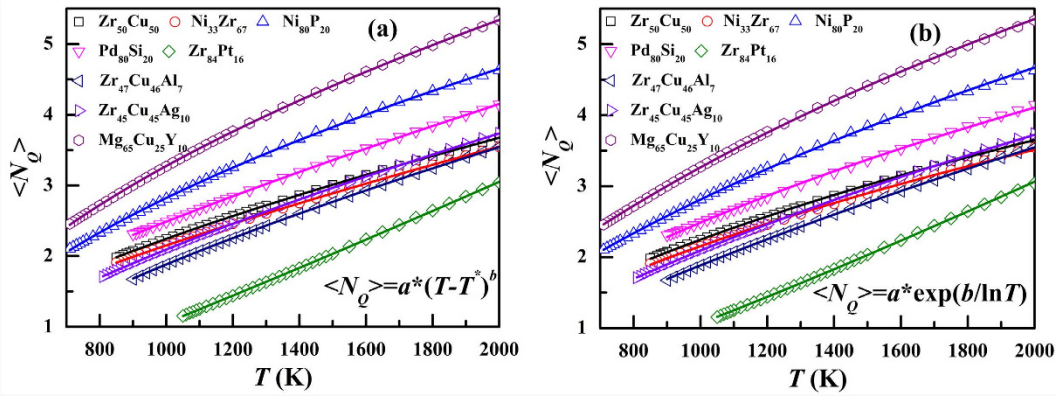

Figure 2. The temperature dependence of $<N_Q>$ in eight systems, the solid curves are the fittings with (**a**) equation (1) and (**b**) equation (2).

Terms	$Zr_{50}Cu_{50}$	$Ni_{33}Zr_{67}$	$Ni_{80}P_{20}$	$Pd_{80}Si_{20}$	$Zr_{84}Pt_{16}$	$Zr_{47}Cu_{46}Al_7$	$Zr_{45}Cu_{45}Ag_{10}$	$Mg_{65}Cu_{25}Y_{10}$
T_g/K	750	700	550	750	900	750	700	550
T_{VFT}/K	647	556	439	672	761	674	593	448
T^*/K	162	55	310	14	381	329	243	297
b	0.63	0.69	0.56	0.73	1.1	0.69	0.69	0.55

Table 1. The characterized temperature for eight systems. T_g is the glass transition temperature. T_{VFT} is the fitting temperature of Vogel-Fulcher-Tammann equation for relaxation time. T^* and b are the fitting parameters in equation (1).

the ideal glass. Thus, T^* should be the ideal glass transition temperature. However, as shown in Table 1, T^* is much lower than the glass transition temperature T_g and even lower than Vogel-Fulcher-Tammann (VFT) temperature[20] for relaxation time, which is thought to be the ideal glass transition temperature. Therefore, although the fitting seems very well, equation (1) might not reflect all the nature of the temperature dependence of N_Q. Similar to viscosity or relaxation time which can be fitted by many equations, $<N_Q>$ might have other good fitting equations. Figure 2(b) displays another fitting equation:

$$<N_Q> = a^* \exp(b/\ln(T)) \quad (2)$$

which has only two parameters, a, and b. It can be found the simulated data are also fitted very well by the equation. However, equation (2) cannot reflect the existence of ideal glass transition. More work will be done to search more reasonable fitting equations in the future.

Spatial distribution of QNA. Figure 3(a,c,e) display the atomic configurations with atoms colored by their N_Q for $Zr_{50}Cu_{50}$, $Ni_{33}Zr_{67}$ and $Ni_{80}P_{20}$ MGs at $T_g + 150$ K. It can be seen that the distribution of N_Q shows clear spatial heterogeneity. The atoms with less N_Q or more N_Q tends to be located together. To quantify the spatial arrangement of N_Q, we calculated a nearest-neighbor correlation index[21,22], $C_{ij} = p_{ij}/p_{ij}^0 - 1$, where p_{ij} and p_{ij}^0 are the probability of atoms with the N_Q types i and j being the nearest neighbors in a structure model and a structure in which the distributions of atoms with different N_Q are spatially uncorrelated, respectively. Therefore, the positive and negative values indicate a preference and an avoiding of atoms with the N_Q types i and j being nearest neighbors, respectively. Figure 3(b,d,f) show the matrix of spatial correlation index C_{ij} of atoms in the liquid structure of $Zr_{50}Cu_{50}$, $Ni_{33}Zr_{67}$ and $Ni_{80}P_{20}$, respectively. Generally in all the three systems, all the atoms are naturally divided into two groups. One is the atoms with small N_Q ($N_Q \leq 2$) and the other one is the atoms with large N_Q ($N_Q > 2$). When atoms belong to the same group, C_{ij} is always positive, indicating that they intend to be nearest neighbors. When atoms belong to different groups, C_{ij} is negative, suggesting that they avoid being nearest neighbors. This fact indicates that QNA does have spatial heterogeneities.

Correlating QNA with potential energy. In Fig. 4, we investigated the correlation between potential energy and N_Q in three models. The distribution of atomic potential energy with different N_Q for Zr and Cu in $Zr_{50}Cu_{50}$ is shown in Fig. 4(a,b), respectively. It can be seen that the distributions with different N_Q have large overlaps, indicating the correlation between N_Q and atomic potential energy is not a one-to-one correspondence. Since the cutoff distance of potential energy is 6.5 Å, much larger that the scale of N_Q, it is reasonable for the large overlaps. However, as shown in the insets of Fig. 4(a,b), atoms with larger N_Q have less negative per-atom potential energy shown. In this respect, N_Q plays an key role in the correlation between local structure and potential energy. This fact suggests that atoms with larger N_Q tend to have lower thermodynamic stability. Figure 4(c,d)

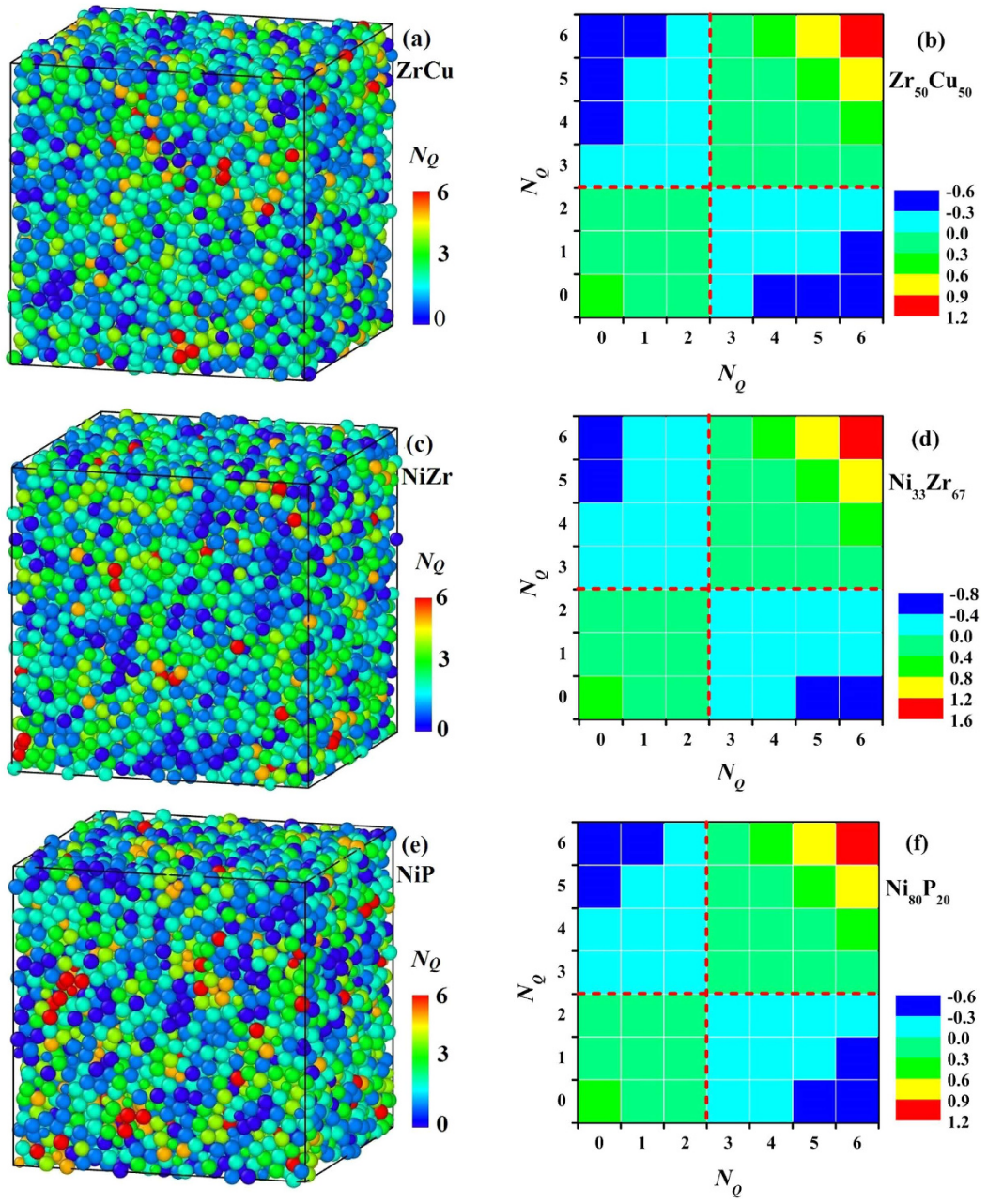

Figure 3. Atom configurations with atoms colored by their N_Q for (**a**) $Zr_{50}Cu_{50}$, (**c**) $Ni_{33}Zr_{67}$ and (**e**) $Ni_{80}P_{20}$ at $T_g + 150$ K. The matrix of spatial correlation index C_{ij} of atoms with different N_Q in (**b**) $Zr_{50}Cu_{50}$, (**d**) $Ni_{33}Zr_{67}$ and (**f**) $Ni_{80}P_{20}$ at $T_g + 150$ K.

shows the results in $Ni_{33}Zr_{67}$ and they are similar to those in $Zr_{50}Cu_{50}$. However, the results in $Ni_{80}P_{20}$, as shown in Fig. 4(e,f) display different features. The distribution of potential energy for Ni with different N_Q is similar to those in Fig. 4(a–d) while that for P is quite different. The distributions of potential energy for P with different N_Q have so large overlaps that all the curves seen to be coincided, suggesting that the correlation between N_Q and atomic potential energy for P atoms is rather weak. Why P atoms show quite different feature? It can be seen in Fig. 1(c) that the atomic packing around P atoms is rather loose. Therefore, the correlation between potential energy and atomic packing might be strong in dense-packing systems such as metallic systems and be weak in the loose-packing systems. That might be the reason why the correlation between N_Q and atomic potential energy for P atoms is rather weak. Therefore, N_Q is more applicable to dense-packing systems.

As indicated in Fig. 4, N_Q displays close correlation with potential energy at the atomic level. In Fig. 5, we investigated the correlation of their average values in eight systems. Strikingly, $<N_Q>$ and per-atom potential energy in all the systems shows simply linear correlation, which suggesting that N_Q plays an important role to link atomic structure and thermodynamic properties.

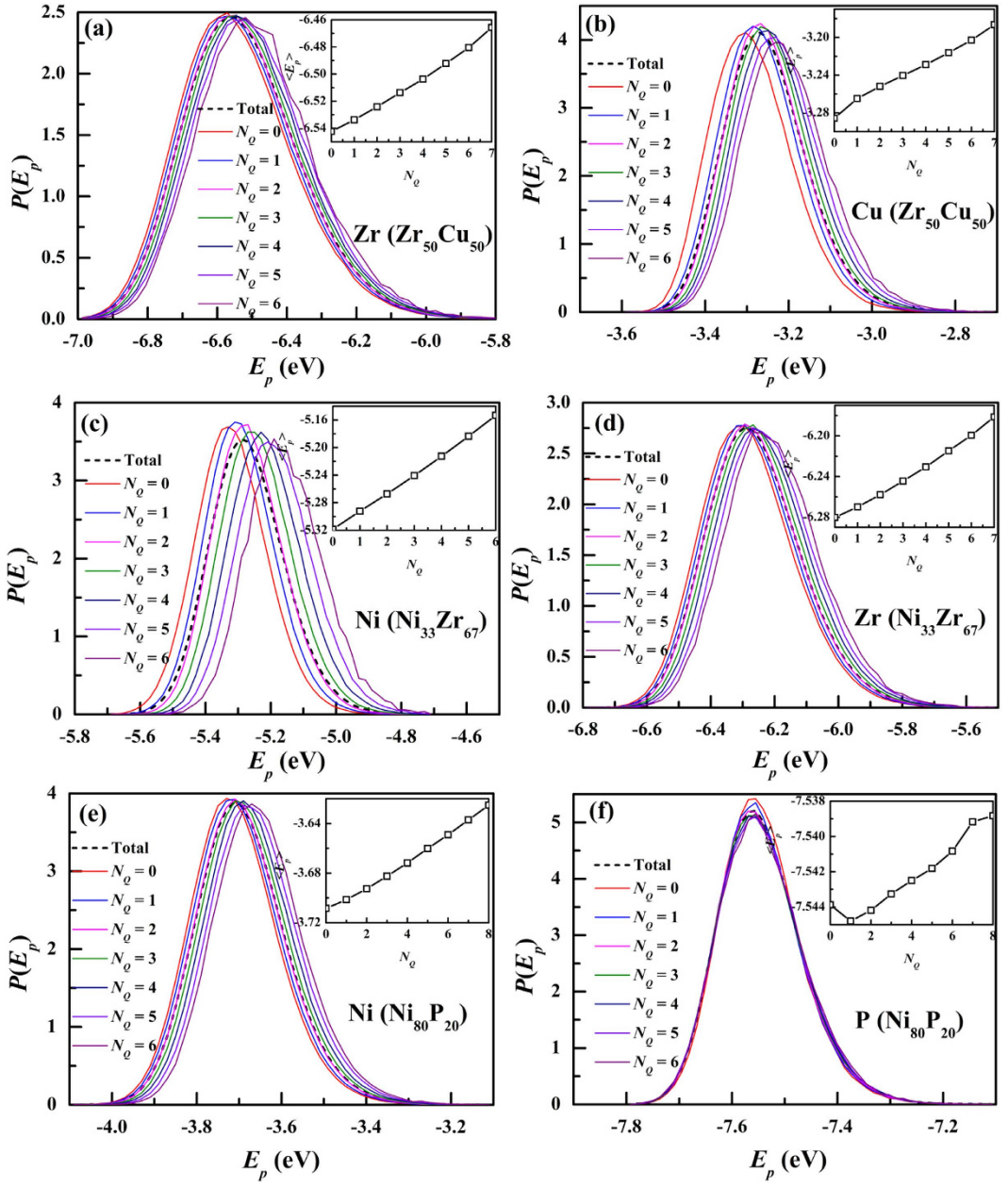

Figure 4. The distribution of potential energy for (**a**) Zr and (**b**) Cu in $Zr_{50}Cu_{50}$, (**c**) Ni and (**d**) Zr in $Ni_{33}Zr_{67}$ as well as (**e**) Ni and (**f**) P in $Ni_{80}P_{20}$ with different N_Q at Tg + 150 K. Insets are the N_Q dependence of the average per-atom potential energy.

Correlating QNA with structure relaxation. We label all the atoms with different N_Q at initial time. We obtain the structural relaxation time for atoms with the same N_Q by calculating the self-intermediate scattering function (SISF)[23],

$$F_s^{ab}(q, t) = \frac{1}{N_{ab}} \sum_{j=1}^{N_{ab}} \langle \exp\{i\vec{q} \cdot [\vec{r}_j(t) - \vec{r}_j(0)]\} \rangle \tag{3}$$

where N_{ab} is the number of type a atoms with $N_Q = b$ at $t = 0$, $\vec{r}$ is the position of each atom, $\vec{q}$ is the wave vector which corresponds to the first peak of the partial structure factor and the average is taken over 100 initial configurations. Figure 6(a,b) display the SISFs of Zr and Cu atoms in $Zr_{50}Cu_{50}$ with different N_Q. In the long-time relaxation (often called α-relaxation) regime, the SISF with small N_Q decays more slowly compared to that with larger N_Q, indicating that atoms with smaller N_Q tend to move slower than those with larger N_Q. The α-relaxation time, τ_α, is defined as the time at which the SISF decays to $1/e$ of its initial value. As shown in the insets, for either component of each system, the relaxation time for atoms decreases with increasing N_Q. Figure 6(c–f) display the SISFs of Ni and Zr atoms in $Ni_{33}Zr_{67}$ as well as Ni and P in $Ni_{80}P_{20}$ with different N_Q. The results show similar trend to

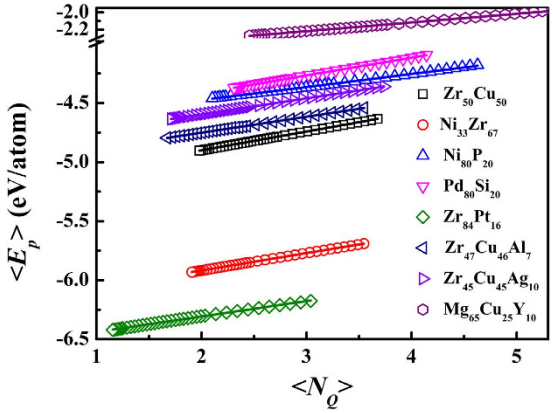

Figure 5. Correlation between $<N_Q>$ and per-atom potential energy in eight systems. The solid curves are the linear fittings.

those in $Zr_{50}Cu_{50}$. It should be noted that the correlation between N_Q and α-relaxation time for P in $Ni_{80}P_{20}$ is much strong. Since the correlation between N_Q and potential energy for P in $Ni_{80}P_{20}$ is rather weak shown in Fig. 4(f), it might be reasonable that the correlation between potential energy and dynamic heterogeneity is much weak, at least weaker than N_Q.

Hu *et al.* proposed an equation to link α-relaxation time and $<1-d5>$ in metallic liquids[24]. We found that the equation can also be used to describe the correlation between $<N_Q>$ and α-relaxation time:

$$\tau_\alpha = \tau_0 \exp(D/<N_Q>^\delta) \quad (4)$$

where τ_0 is the relaxation time at infinite liquidus temperature, and δ and D are fitting parameters. Figure 7 illustrates the α-relaxation time τ_α as a function of $<N_Q>$ and the fittings of equation (4) for various metallic liquids ($R^2 > 0.99$ for all the fittings). Remarkably, equation (4) can well describe the relationship between α-relaxation time and $<N_Q>$ in these metallic liquids. In addition, δ is fitted to be about 3.36, 3.99, 2.76, 5.26, 2.22, 3.85, 3.49, and 2.90 for $Zr_{50}Cu_{50}$, $Ni_{33}Zr_{67}$, $Ni_{80}P_{20}$, $Pd_{80}Si_{20}$, $Zr_{84}Pt_{16}$, $Zr_{47}Cu_{46}Al_7$, $Zr_{45}Cu_{45}Ag_{10}$ and $Mg_{65}Cu_{25}Y_{10}$ metallic liquids, respectively. Clearly, δ is similar for different systems. δ reflects the sensitivity of α-relaxation time to the change of $<N_Q>$. Therefore, the effect of the $<N_Q>$ change on the structure relaxation is similar in different metallic liquids.

Conclusion

In this work, we study the salient characteristics of structural disorder in metallic liquids employing a new descriptor of local structure, quasi-nearest atom (QNA). By calculating the number of QNAs (N_Q) for each atom, we can quantify the degree of atomic packing of an individual atom. From the present analysis, the scaled distribution of N_Q, appears to be universal in metallic liquids. The QNA can be correlated with local potential energy and successively with dynamical properties (structural relaxation) at the atomic level. Some straightforward relationships have been proposed to reflect the correlations between QNA and other properties from the macroscopical view. These correlations indicate that the QNA is an important structural identifier that can accurately quantify the local packing and shed light on the structure-property relationship.

Although QNA shows close correlation with some properties in metallic liquids, we noted that it is only a crude measure of how regular the short-range packing order is, and it reflects some information already carried by the Voronoi index. In terms of insight, our results are expected: the larger N_Q is, the worse the local packing order is, the further away from the preferred and best-ordered Kasper polyhedra, the more likely that they are of higher potential energy, and the higher likelihood for them to participate in relaxation and diffusion.

Method

Classical molecular dynamics simulations are carried out on eight model systems ($Zr_{50}Cu_{50}$, $Ni_{33}Zr_{67}$, $Ni_{80}P_{20}$, $Pd_{80}Si_{20}$, $Zr_{84}Pt_{16}$, $Zr_{47}Cu_{46}Al_7$, $Zr_{45}Cu_{45}Ag_{10}$ and $Mg_{65}Cu_{25}Y_{10}$) of metallic glass-forming liquids through LAMMPS[25] with the embedded atom method (EAM) potential[26–33]. For each model, a cubic simulation box containing 10,000 atoms, with periodic boundary conditions applied in all dimensions, was equilibrated through isothermal-isobaric (*NPT*) simulations ($P = 0$) for enough time to make sure that the potential energy keeps dynamically equilibrated. Pressure and temperature oscillations were controlled through a Nose-Hoover barostat and thermostat, respectively. The equations of motion are integrated using the Verlet algorithm with a time step of 1 fs. The configuration at 2000 K is a random one and Each successive T is based on the final of the previous T. At each temperature, the initial configuration was relaxed for enough time to make sure that the potential energy of the system reaches dynamically equilibrated. At each temperature of interest, the equilibrated configurations were run for 1 ns (high temperatures) or 10 ns (low temperatures). 1000 configurations were collected for structure analysis and 100 initial configurations were used to calculate dynamical properties. Voronoi polyhedron analysis was performed to describe the atomic structure in metallic liquids. The Voronoi polyhedral index is expressed as

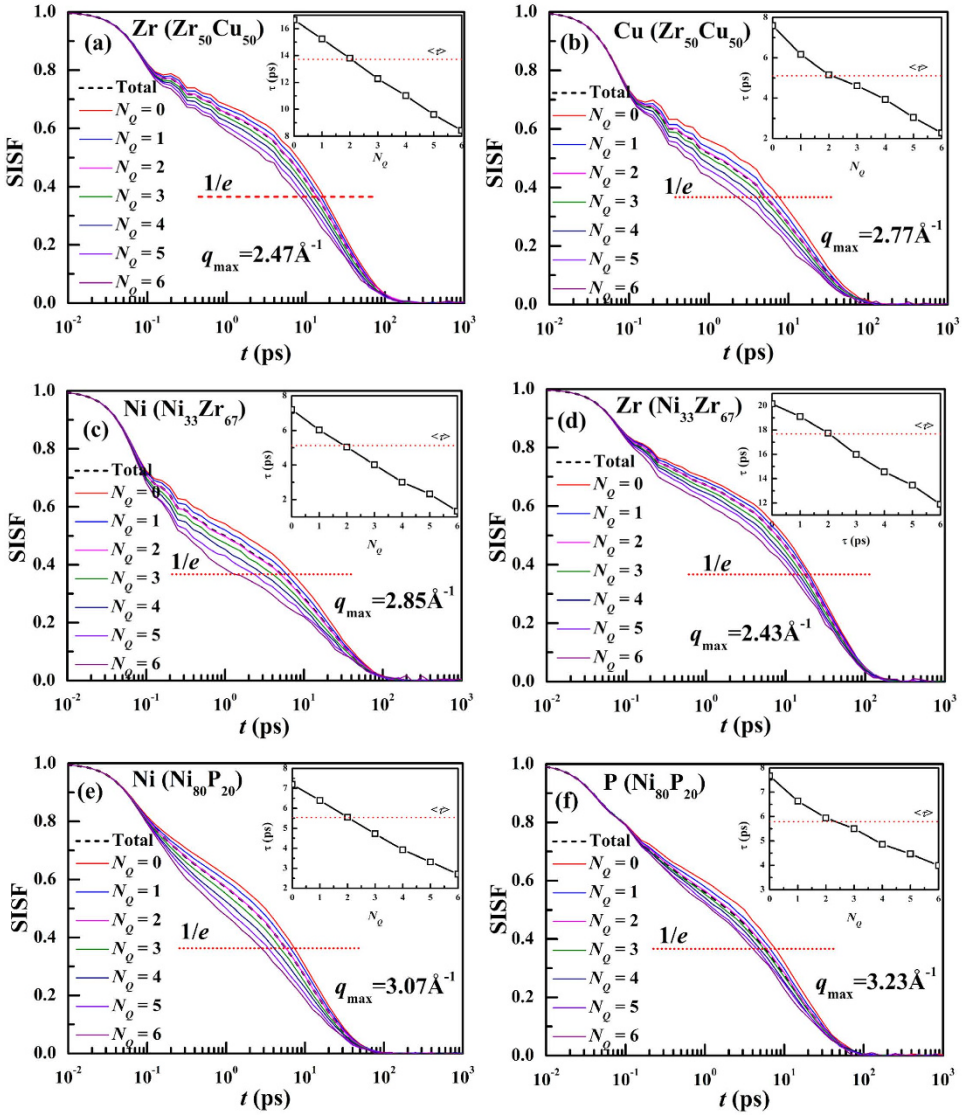

Figure 6. Self-intermediate scattering functions of (**a**) Zr and (**b**) Cu in $Zr_{50}Cu_{50}$, (**c**) Ni and (**d**) Zr in $Ni_{33}Zr_{67}$ as well as (**e**) Ni and (**f**) P in $Ni_{80}P_{20}$ with different N_Q at the initial time at Tg + 150 K. Insets in (**a~f**) are the N_Q-dependence of relaxation times and the dash line corresponds to the relaxation time for the element. 100 initial configurations were used to calculate SISFs.

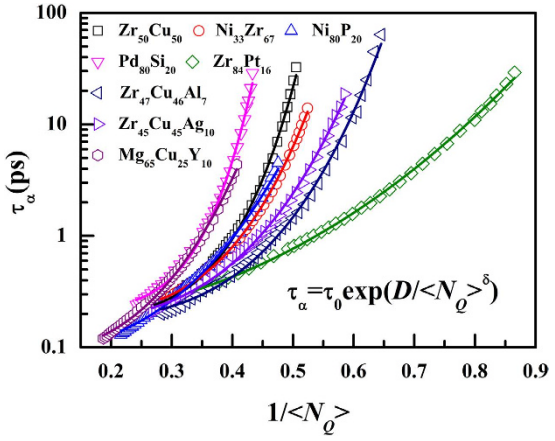

Figure 7. Correlation between $<N_Q>$ and α-relaxation time in eight systems. The solid curves are the fittings with equation (4).

$<n_3, n_4, n_5, n_6>$, where n_i denotes the number of i-edged faces of the Voronoi polyhedron. Further analysis based on Voronoi polyhedron was performed to calculating the number of QNAs (N_Q) for each atom[32]. More details on the definition of QNA can be found in the supplemental material.

References

1. Liu, X. J. *et al.* Metallic liquids and glasses: atomic order and global packing. *Phys. Rev. Lett.* **105,** 155501 (2010).
2. Ma, E. Tuning order in disorder. *Nat. Mater.* **14,** 547–552 (2015).
3. Pan, S., Feng, S., Qiao, J., Dong, B. & Qin, J. The atomic structure of liquid Fe–C alloys. *J. Alloys Compd.* **648,** 178–183 (2015).
4. Wu, C. *et al.* A metric to gauge local distortion in metallic glasses and supercooled liquids. *Acta Mater.* **72,** 229–238 (2014).
5. Fang, X., Wang, C., Yao, Y., Ding, Z. & Ho, K. Atomistic cluster alignment method for local order mining in liquids and glasses. *Phys. Rev. B* **82,** 184204 (2010).
6. Pan, S., Qin, J., Wang, W. & Gu, T. A new method to characterize medium range order in metallic glasses. *J. Non-Cryst. Solids* **358,** 1873–1875 (2012).
7. Ediger, M. & Harrowell, P. Perspective: Supercooled liquids and glasses. *J. Chem. Phys.* **137,** 080901 (2012).
8. Cheng, Y. & Ma, E. Atomic-level structure and structure–property relationship in metallic glasses. *Prog. Mater. Sci.* **56,** 379–473 (2011).
9. Huang, L., Wang, C., Hao, S., Kramer, M. & Ho, K. Atomic size and chemical effects on the local order of Zr 2 M (M = Co, Ni, Cu, and Ag) binary liquids. *Phys. Rev. B* **81,** 014108 (2010).
10. Widmer-Cooper, A. & Harrowell, P. Predicting the long-time dynamic heterogeneity in a supercooled liquid on the basis of short-time heterogeneities. *Phys. Rev. Lett.* **96,** 185701 (2006).
11. Widmer-Cooper, A., Perry, H., Harrowell, P. & Reichman, D. R. Irreversible reorganization in a supercooled liquid originates from localized soft modes. *Nat. Phys.* **4,** 711–715 (2008).
12. Ding, J., Patinet, S., Falk, M. L., Cheng, Y. & Ma, E. Soft spots and their structural signature in a metallic glass. *Proc. Natl. Acad. Sci.* **111,** 14052–14056 (2014).
13. Cohen, M. H. & Grest, G. Liquid-glass transition, a free-volume approach. *Phys. Rev. B* **20,** 1077 (1979).
14. Starr, F. W., Sastry, S., Douglas, J. F. & Glotzer, S. C. What do we learn from the local geometry of glass-forming liquids? *Phys. Rev. Lett.* **89,** 125501 (2002).
15. Widmer-Cooper, A. & Harrowell, P. Free volume cannot explain the spatial heterogeneity of Debye–Waller factors in a glass-forming binary alloy. *J. Non-Cryst. Solids* **352,** 5098–5102 (2006).
16. Wen, P., Zhao, Z. F., Pan, M. X. & Wang, W. H. Mechanical relaxation in supercooled liquids of bulk metallic glasses. *Phys. Status Solidi A* **207,** 2693–2703 (2010).
17. Pan, S., Feng, S., Qiao, J., Wang, W. & Qin, J. Correlation between local structure and dynamic heterogeneity in a metallic glass-forming liquid. *J. Alloys Compd.* **664,** 65–70 (2016).
18. Cheng, Y., Sheng, H. & Ma, E. Relationship between structure, dynamics, and mechanical properties in metallic glass-forming alloys. *Phys. Rev. B* **78,** 014207 (2008).
19. Yu, H., Richert, R., Maaß, R. & Samwer, K. Unified Criterion for Temperature-Induced and Strain-Driven Glass Transitions in Metallic Glass. *Phys. Rev. Lett.* **115,** 135701 (2015).
20. Angell, C. A., Ngai, K. L., McKenna, G. B., McMillan, P. F. & Martin, S. W. Relaxation in glassforming liquids and amorphous solids. *J. Appl. Phys.* **88,** 3113–3157 (2000).
21. Li, M., Wang, C., Hao, S., Kramer, M. & Ho, K. Structural heterogeneity and medium-range order in Zr x Cu 100− x metallic glasses. *Phys. Rev. B* **80,** 184201 (2009).
22. Peng, H., Li, M., Wang, W., Wang, C.-Z. & Ho, K. Effect of local structures and atomic packing on glass forming ability in CuxZr100− x metallic glasses. *Appl. Phys. Lett.* **96,** 021901 (2010).
23. Kob, W. & Andersen, H. C. Testing mode-coupling theory for a supercooled binary Lennard-Jones mixture. II. Intermediate scattering function and dynamic susceptibility. *Phys. Rev. E* **52,** 4134 (1995).
24. Hu, Y., Li, F., Li, M., Bai, H. & Wang, W. Five-fold symmetry as indicator of dynamic arrest in metallic glass-forming liquids. *Nat. Commun.* **6** (2015).
25. Plimpton, S. Fast parallel algorithms for short-range molecular dynamics. *J. Comp. Phys.* **117,** 1–19 (1995).
26. Cheng, Y., Ma, E. & Sheng, H. Atomic level structure in multicomponent bulk metallic glass. *Phys. Rev. Lett.* **102,** 245501 (2009).
27. Mendelev, M., Kramer, M., Hao, S., Ho, K. & Wang, C. Development of interatomic potentials appropriate for simulation of liquid and glass properties of NiZr2 alloy. *Phil. Mag.* **92,** 4454–4469 (2012).
28. Sheng, H., Ma, E. & Kramer, M. J. Relating dynamic properties to atomic structure in metallic glasses. *JOM* **64,** 856–881 (2012).
29. Ding, J., Cheng, Y.-Q., Sheng, H. & Ma, E. Short-range structural signature of excess specific heat and fragility of metallic-glass-forming supercooled liquids. *Phys. Rev. B* **85,** 060201 (2012).
30. Hirata, A. *et al.* Geometric frustration of icosahedron in metallic glasses. *Science* **341,** 376–379 (2013).
31. Fujita, T. *et al.* Coupling between chemical and dynamic heterogeneities in a multicomponent bulk metallic glass. *Phys. Rev. B* **81,** 140204 (2010).
32. Ding, J., Cheng, Y. & Ma, E. Charge-transfer-enhanced prism-type local order in amorphous Mg 65 Cu 25 Y 10: Short-to-medium-range structural evolution underlying liquid fragility and heat capacity. *Acta Mater.* **61,** 3130–3140 (2013).
33. Medvedev, N. The algorithm for three-dimensional Voronoi polyhedra. *J. Comput. Phys.* **67,** 223–229 (1986).

Acknowledgements

This work was supported by the National Natural Science Foundation of China (Grant Nos 51571132, 51304145, 51271162, 51501043 and 51574176) and the Program for the Innovative Talents of Higher Learning Institutions of Shanxi (Grant No. 143020142–S, 2014jytrc04).

Author Contributions

S.-P.P. and J.-Y.Q. conceived the project and wrote manuscript. S.-P.P. and S.-D.F. performed the molecular dynamics simulations. S.-P.P., S.-D.F., L.-M.W., J.-W.Q., X.-F.N., B.-S.D., W.-M.W. and J.-Y.Q. analyzed the data. All authors reviewed the manuscript.

Additional Information

Supplementary information accompanies this paper at http://www.nature.com/srep

Competing financial interests: The authors declare no competing financial interests.

How to cite this article: Pan, S.-P. *et al.* Structural disorder in metallic glass-forming liquids. *Sci. Rep.* **6**, 27708; doi: 10.1038/srep27708 (2016).